Prospect on constraining string-theory-inspired model from gravitational redshift measurements

胡立

Li Hu

Institute of Theoretical Physics, Chinese Academy of Sciences
Hangzhou Institute for advanced study, UCAS

2025 Gravitational Wave Physics Conference

2025-10-18 @ ITP, Chun'an @ 15:00-15:20

Modified Gravity

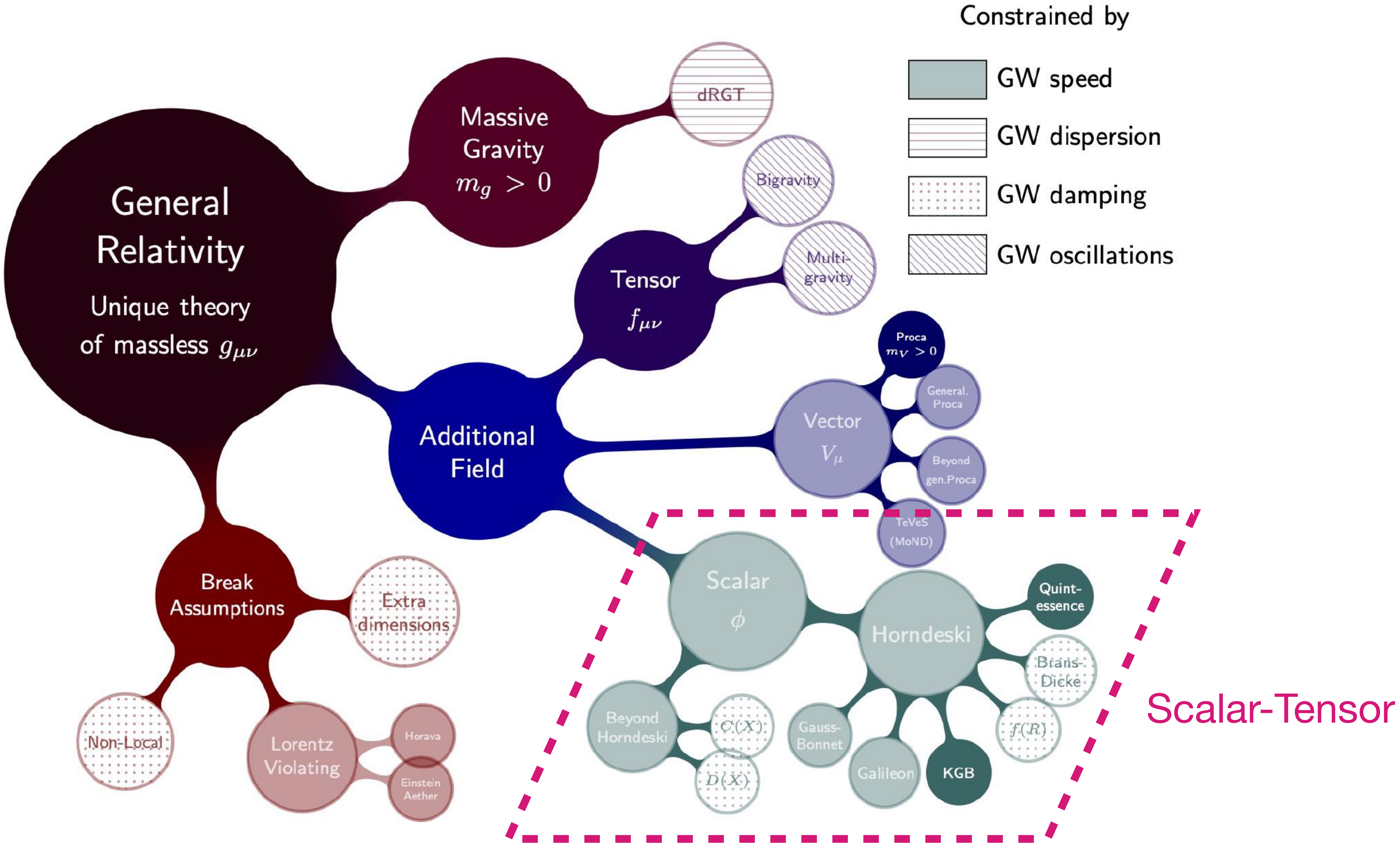

Existing tests

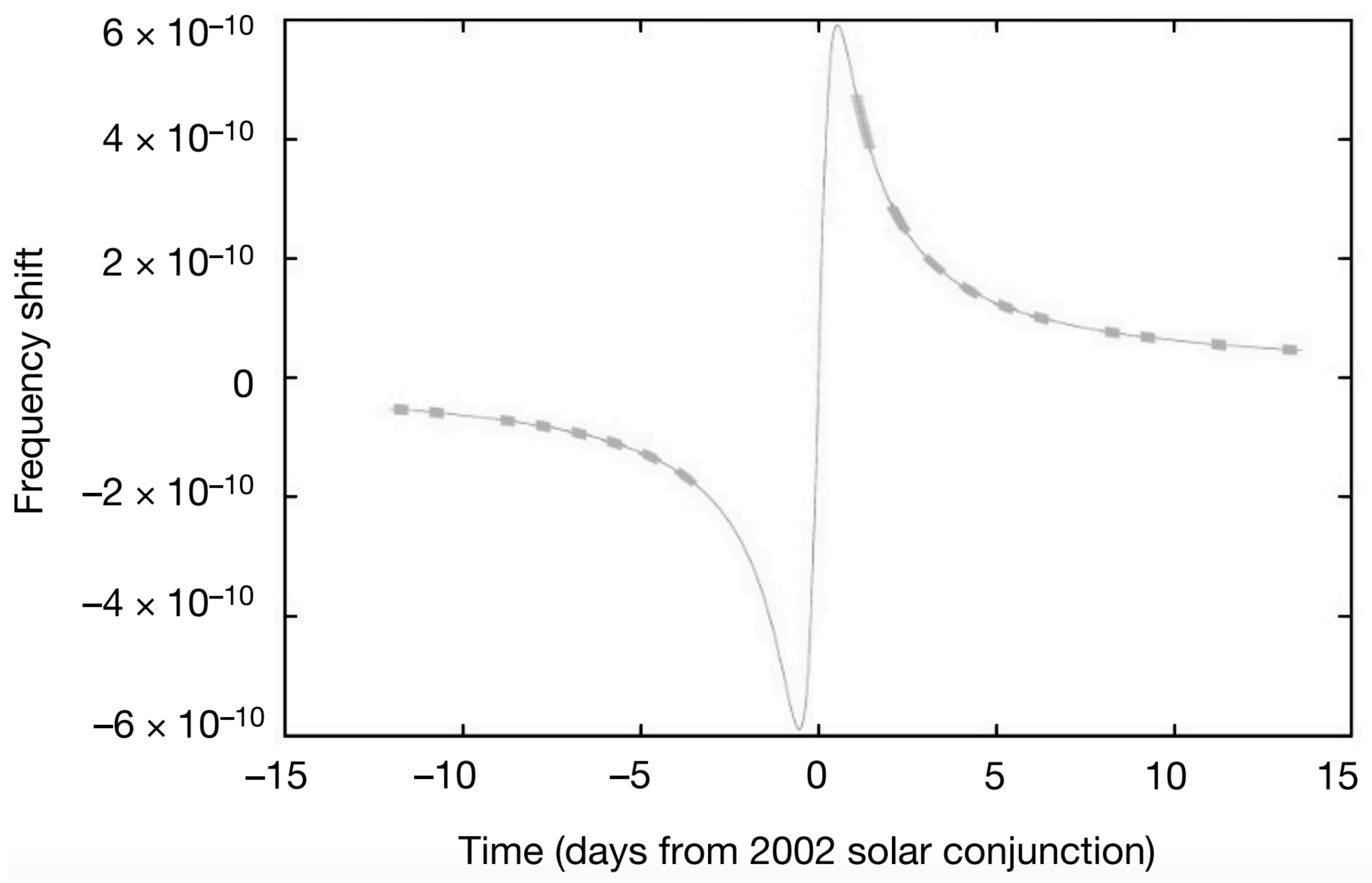

Bertotti, Iess, Tortora 2003 Nature

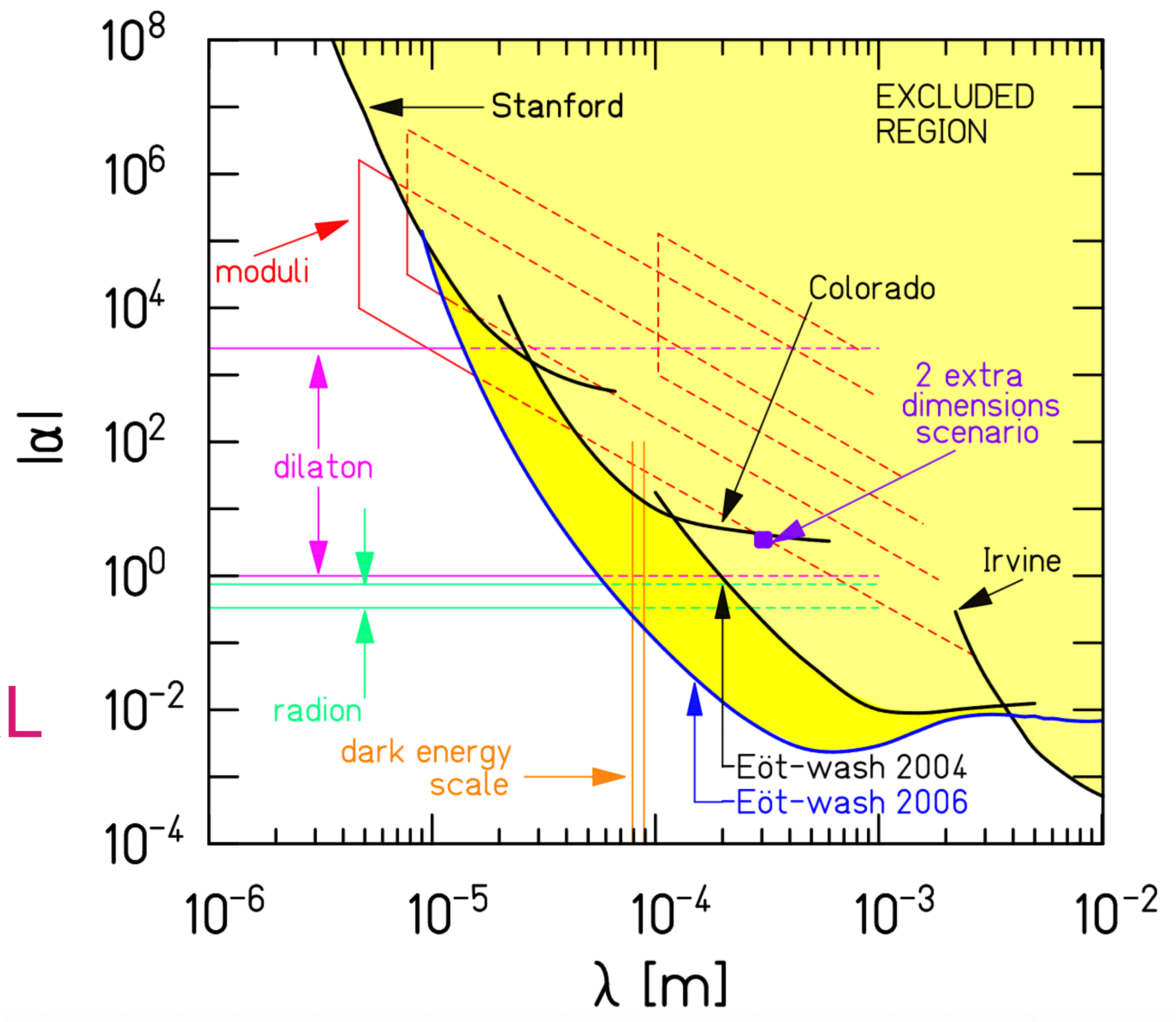

Kapner et.al 2007 PRL

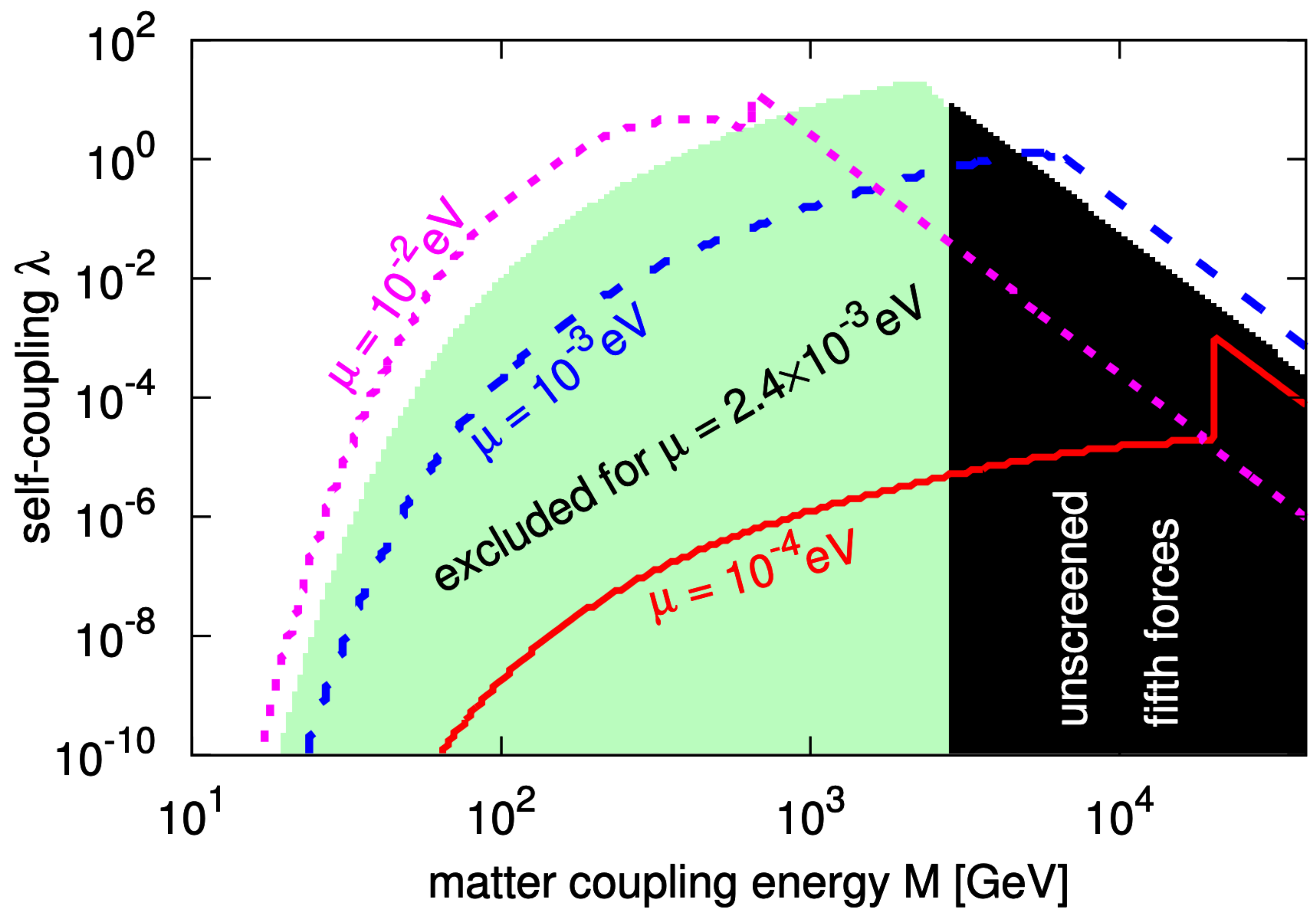

Upadhye 2013 PRL

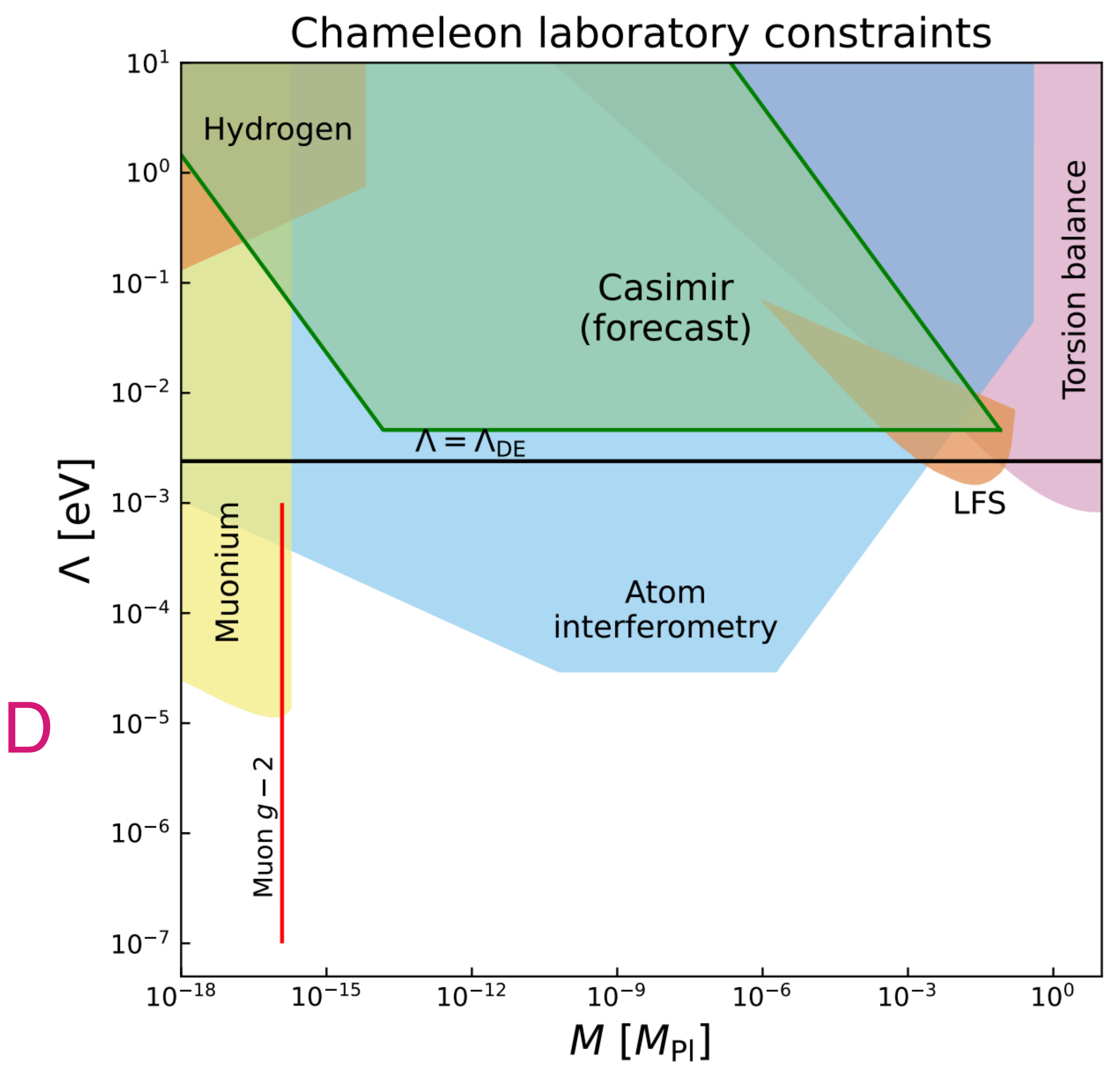

Brax, Davis, Elder 2023 PRD

Screening mechanisms

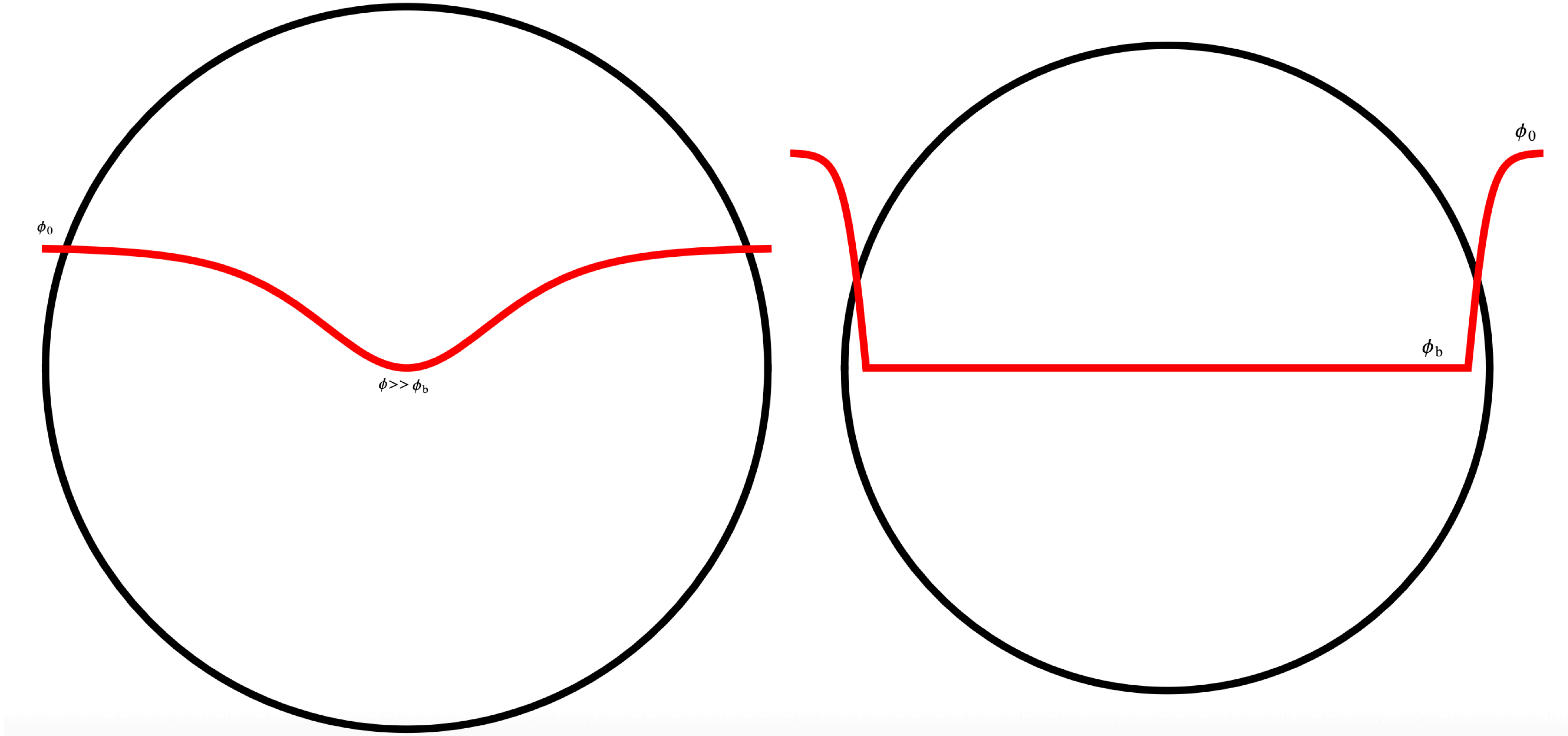

Unscreened

Screened

Chameleon

Symmetron

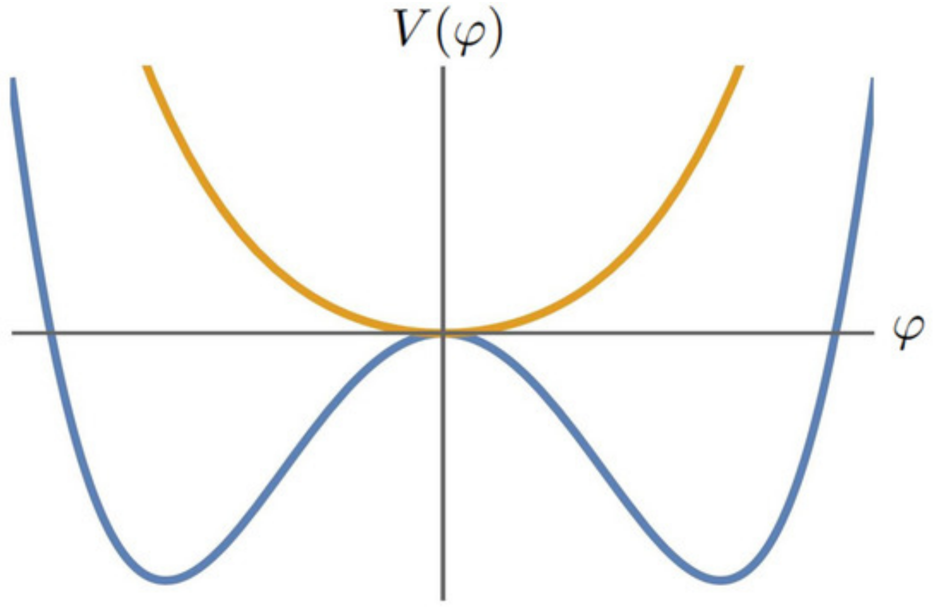

Damour–Polyakov effect

Vainshtein mechanism

Dilaton

Jordan frame

[Brax et.al 2010 PRD]

$$S=\int\sqrt{-\tilde{g}}\,\mathrm{d}^4x\left[\frac{e^{-2\psi(\phi)}}{2l_s^2}\tilde{R}+\frac{Z(\phi)}{2l_s^2}(\tilde{\nabla}\phi)^2-\tilde{V}(\phi)\right]+S_{\mathrm{mat}}(\tilde{g}_{\mu\nu},\Psi_i;g_i(\phi))\,,$$

Einstein frame

$\phi\to\infty$

$$G_{\mu\nu}\equiv R_{\mu\nu}-\frac{1}{2}Rg_{\mu\nu}=\frac{1}{M_{\mathrm{pl}}^2}(T_{\mu\nu}+T_{\mu\nu}^{(\phi)})\,,$$

$$\Box\phi\equiv g^{\mu\nu}\nabla_\mu\nabla_\nu\phi=\frac{\mathrm{d}V}{\mathrm{d}\phi}+\frac{\mathrm{d}\ln A}{\mathrm{d}\phi}\rho\,.$$

Newtonian Limit

$$2M_{\mathrm{pl}}^2\Delta\Phi=\rho-2V(\varphi)\,,$$

$$\Delta\varphi=\frac{\mathrm{d}V_{\mathrm{eff}}(\varphi)}{\mathrm{d}\varphi}=-\frac{V_0}{M_{\mathrm{Pl}}}+\frac{A_2(\rho+4V_0)}{M_{\mathrm{Pl}}^2}\varphi\,.$$

$$V_{\mathrm{eff}}(\varphi)=V_0-V_0\left(\frac{\varphi}{M_{\mathrm{Pl}}}\right)+\frac{A_2}{2}(\rho+4V_0)\left(\frac{\varphi}{M_{\mathrm{Pl}}}\right)^2.$$

$$A(\phi)=1+\omega(\phi)=1+\frac{A_2}{2M_{\mathrm{pl}}^2}(\phi-\phi_*)^2\,,$$

$$\varphi_{\mathrm{min}}=\frac{V_0M_{\mathrm{Pl}}}{A_2(4V_0+\rho)}\,.$$

[Brax, Davis, Jha 2017 PRD]

Force vs Potential

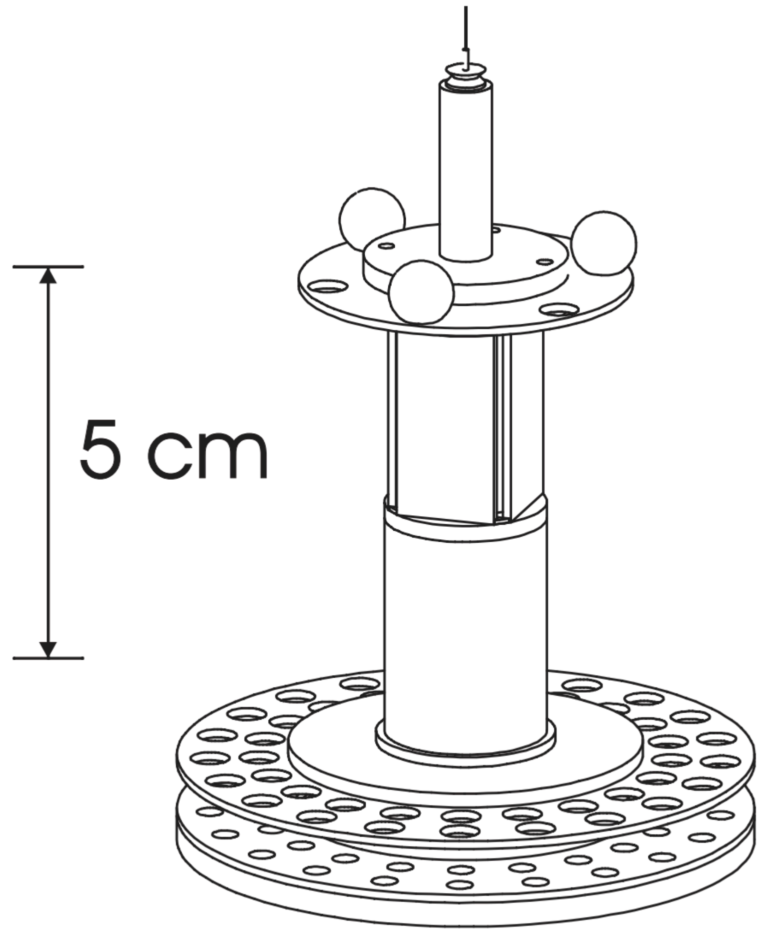

Kapner et.al 2007 PRL

	5^{th} force effects "$\nabla[\ln\Omega(\phi)]$"	Potential effects "$\ln\Omega(\phi)$"
Classical probe	torsion balance [24–27], galaxy dynamics [36, 37]	gravitational redshift
Quantum probe	atom interferometry [31–34]	atomic levels [43, 44], bouncing neutron [45–48]

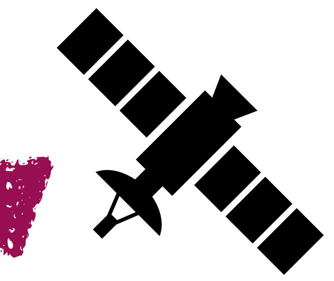

Levy & Uzan 2025 PRD

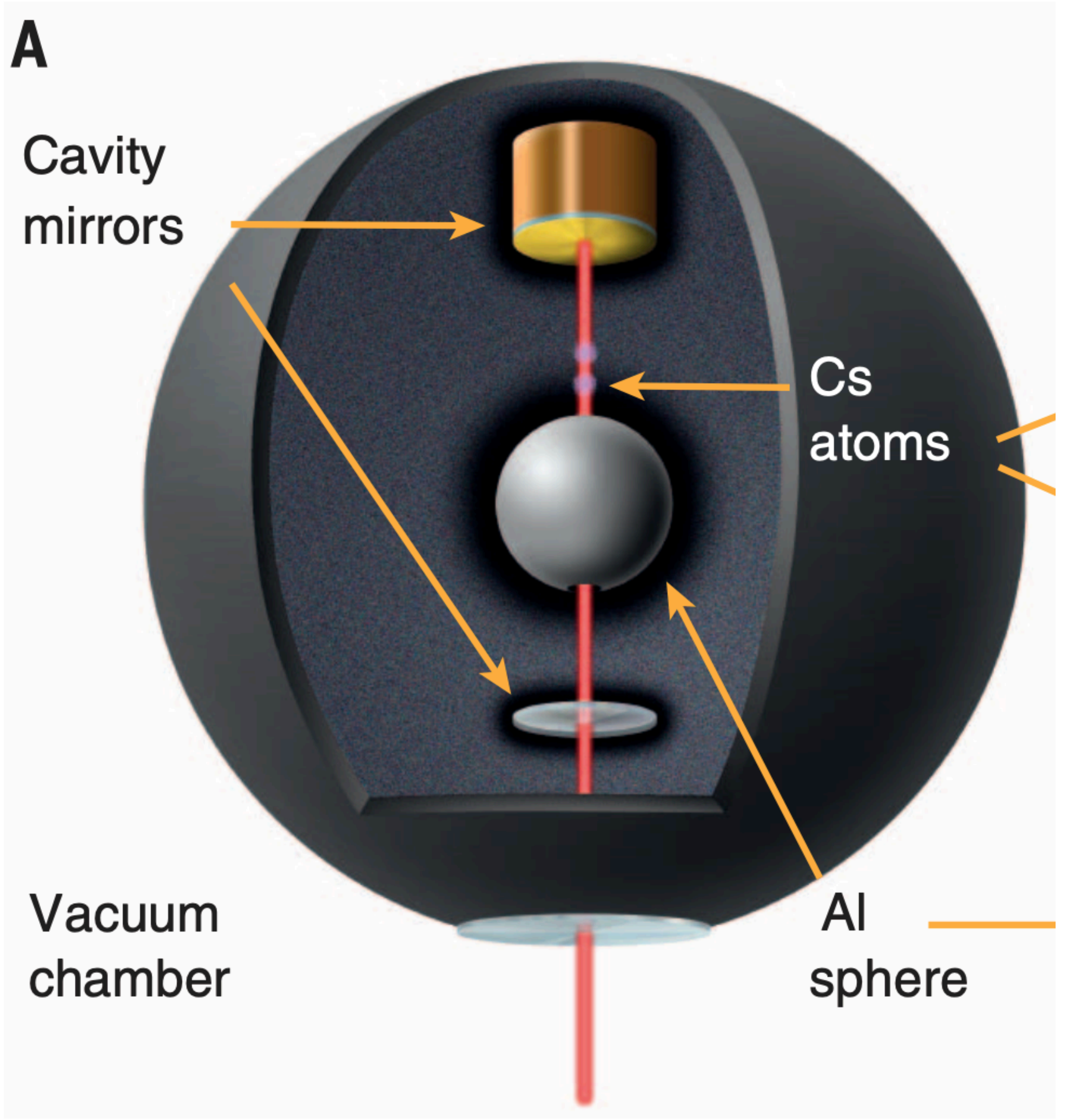

Hamilton et.al, 2015 Science

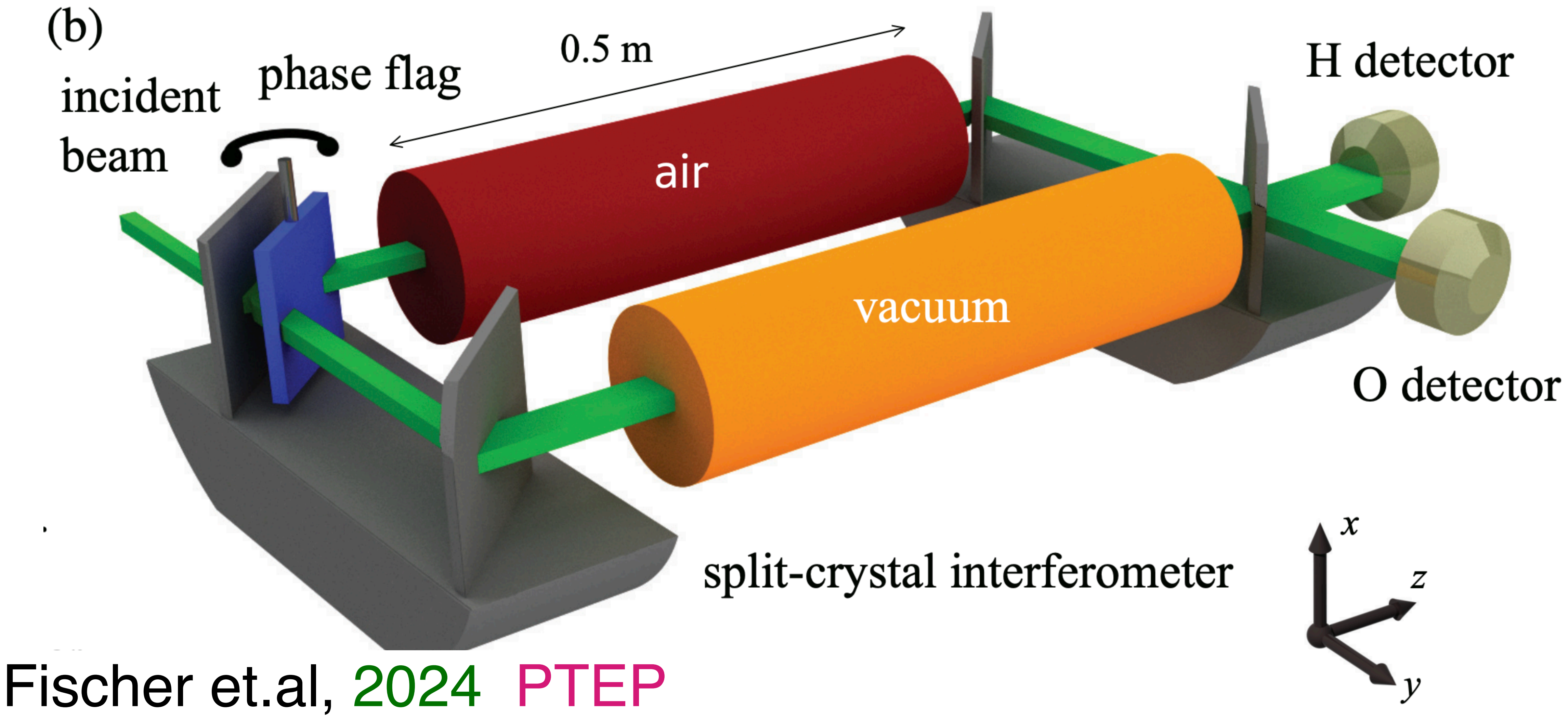

Fischer et.al, 2024 PTEP

Gravitational redshift

Jordan frame

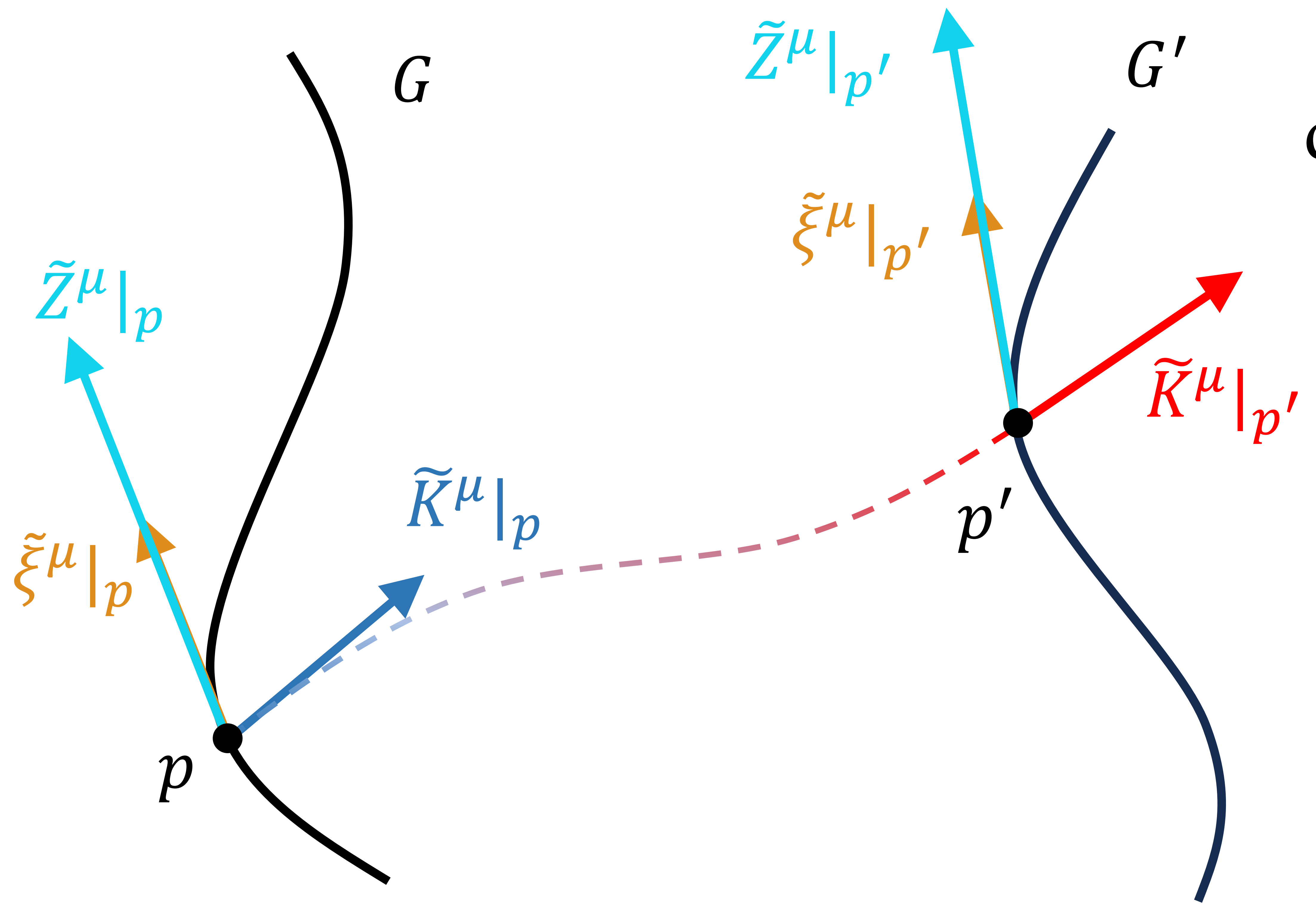

$$1 + z \equiv \frac{E|_p}{E|_{p'}} = \frac{[-(\tilde{K}_\mu \tilde{\xi}^\mu)\zeta^{-1}]|_p}{[-(\tilde{K}_\mu \tilde{\xi}^\mu)\zeta^{-1}]|_{p'}} = \frac{\sqrt{-\tilde{g}_{00}}|_{p'}}{\sqrt{-\tilde{g}_{00}}|_p}.$$

Newtonian limit

$$d\tilde{s}^2 = -(1 + 2\tilde{\Phi})dt^2 + (1 - 2\tilde{\Phi})(dx^2 + dy^2 + dz^2)$$

$$z = \sqrt{\frac{1 + 2\tilde{\Phi}|_{p'}}{1 + 2\tilde{\Phi}|_p}} - 1$$

$$\approx [\Phi + \omega(\phi)]|_{p'} - [\Phi + \omega(\phi)]|_p.$$

$$z_\phi = \omega(\phi)|_{p'} - \omega(\phi)|_p.$$

Continuous model

Continuous

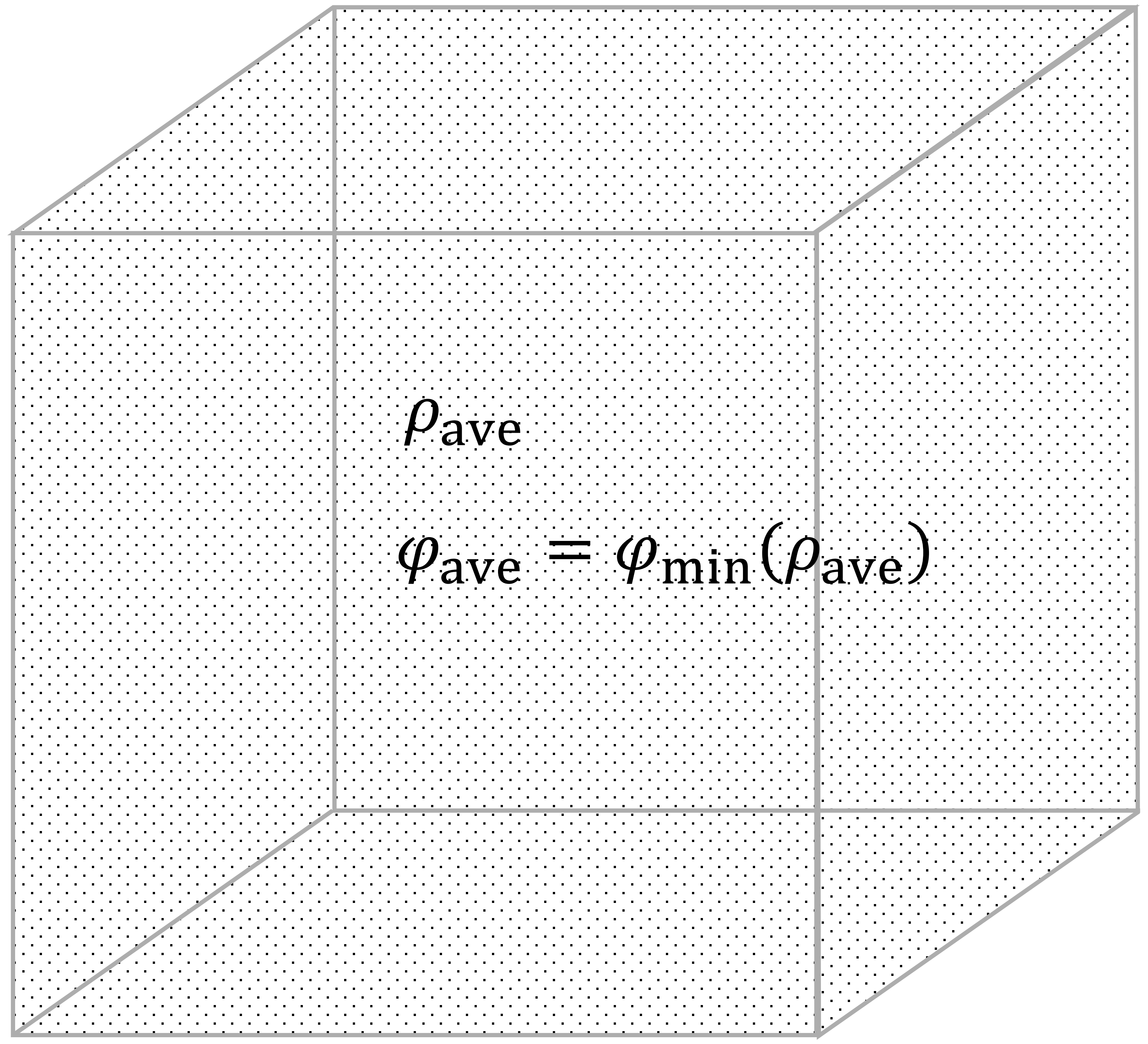

$$z_\phi = \frac{V_0^2}{2A_2}\left[\left(\frac{1}{4V_0 + \rho_{1,\mathrm{ave}}}\right)^2 - \left(\frac{1}{4V_0 + \rho_{2,\mathrm{ave}}}\right)^2\right],$$

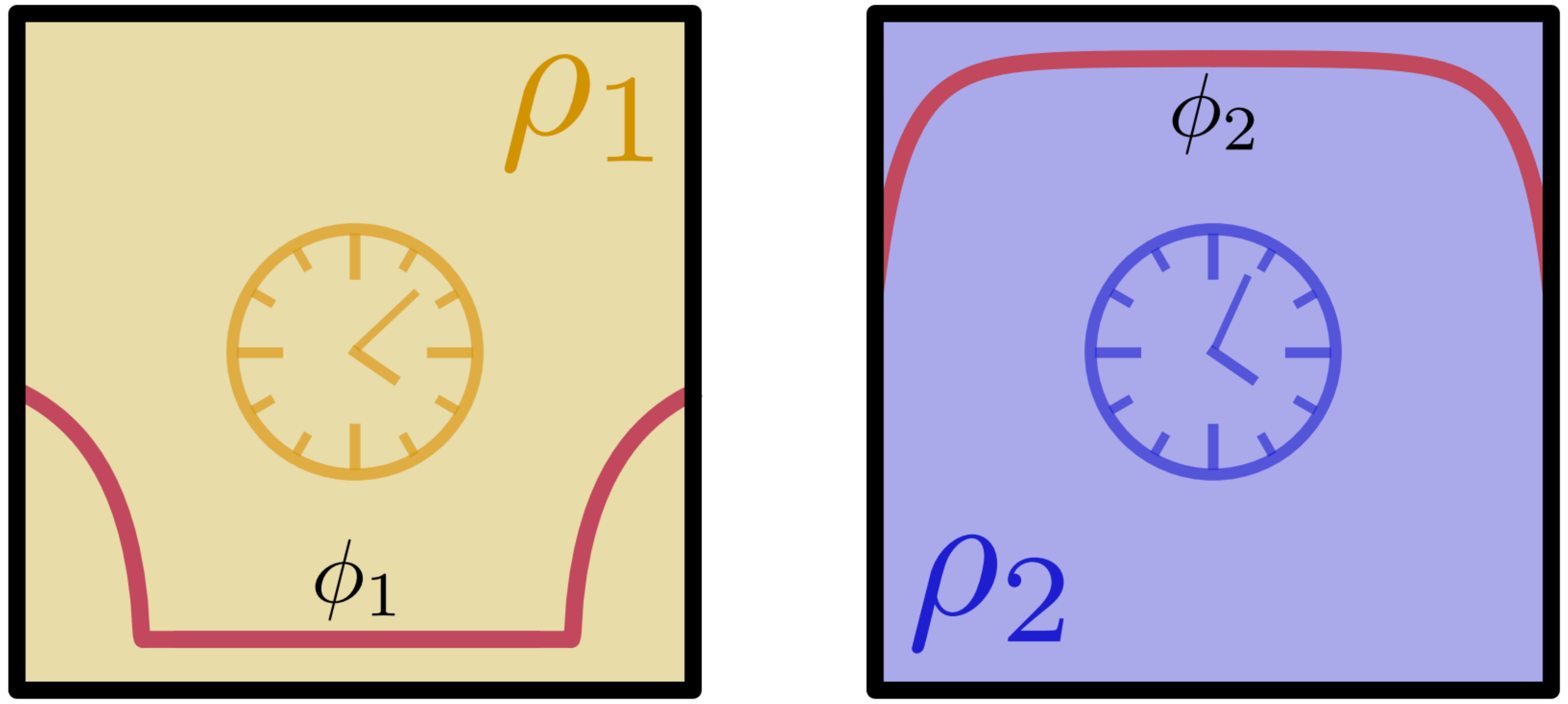

$$z = \frac{f}{f'} - 1\,.$$

Material	Osmium	Water	Air	Dilute gas	UHV	XHV	IPM
Mean density $\rho_{\rm ave}(\mathrm{kg/m^3})$	2.26×10^4	10^3	4.2	4.2×10^{-3}	4.2×10^{-9}	4.2×10^{-15}	4.2×10^{-21}

Ideal experiment

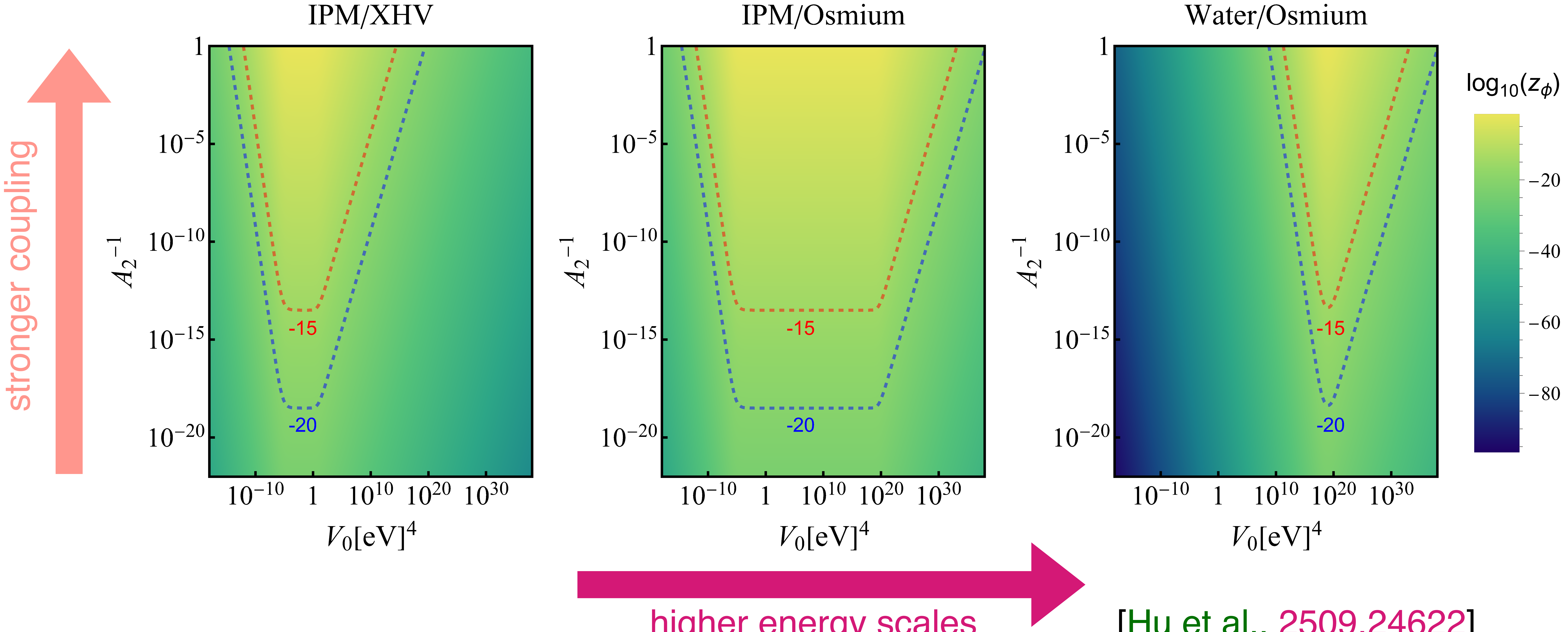

[Hu et al., 2509.24622]

Actual experiment

excluded by environment

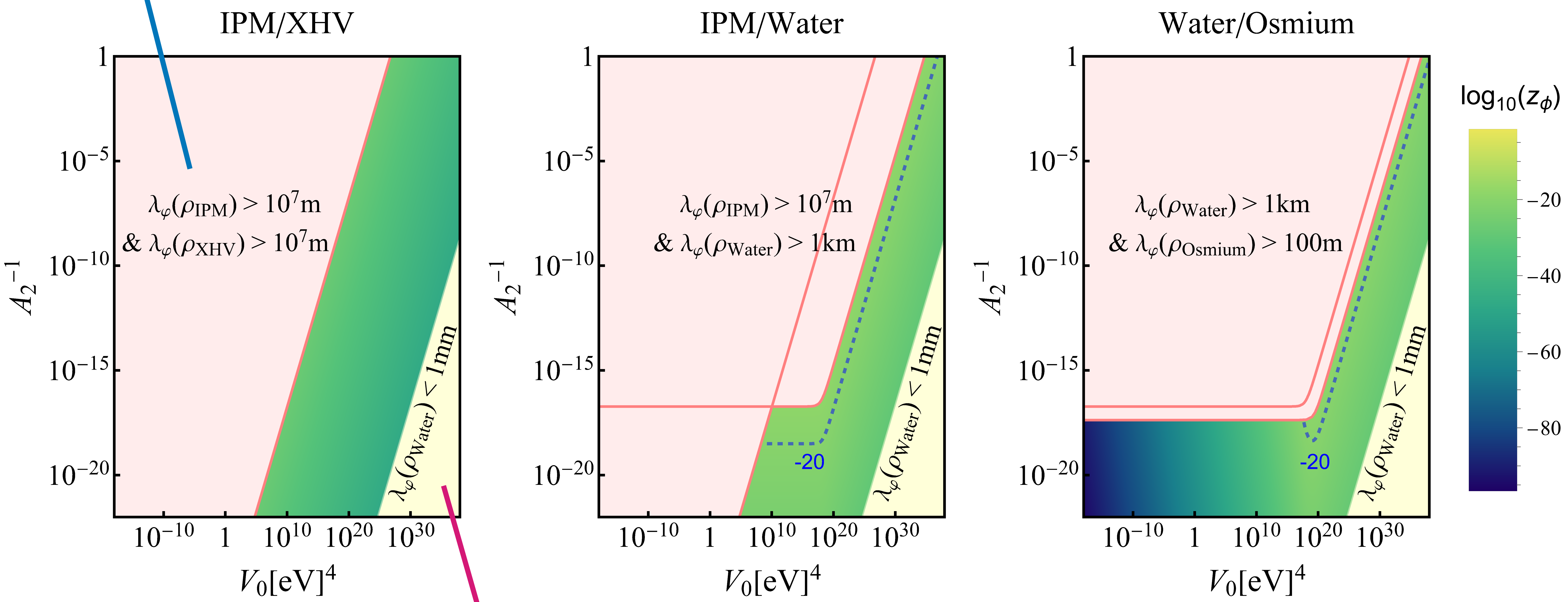

excluded by shell

[Hu et al., 2509.24622]

Discrete model

Discrete

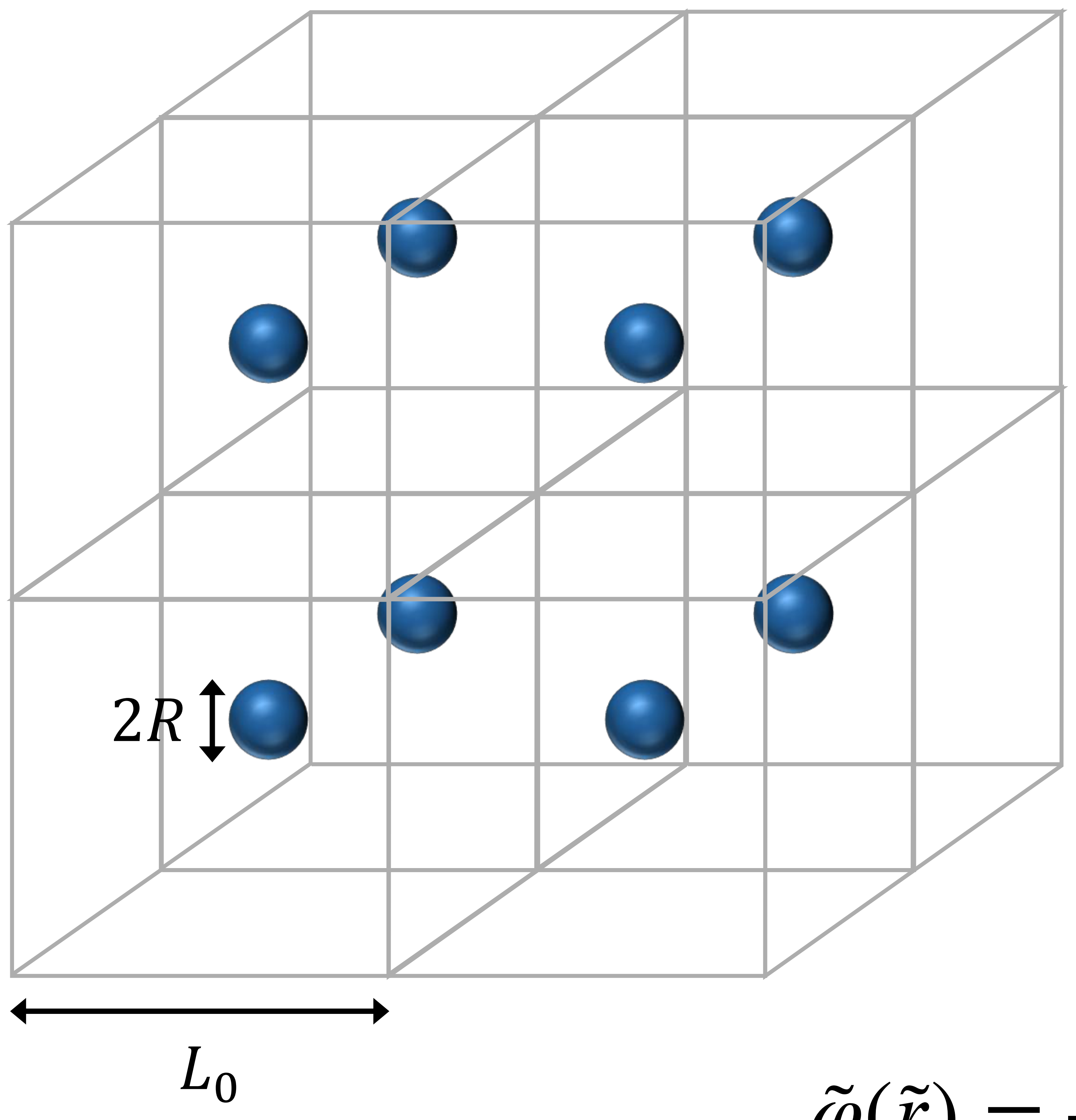

$$\eta\tilde{\Delta}\tilde{\varphi} = -(\xi + 1) + \tilde{\varphi}(\xi + \tilde{\rho})\,.$$

approximate spherical symmetry

modified Bessel equation

$$\tilde{\varphi}(\tilde{r}) = \frac{F(\frac{1}{k_1^2} - \frac{1}{k_2^2})}{\frac{\sinh u}{u} + \frac{k_2}{k_1}\frac{u\cosh u - \sinh u}{v(v+1)}}\frac{\sinh(k_1\tilde{r})}{k_1\tilde{r}} - \frac{F}{k_1^2}\,, \qquad \tilde{r} \le \tilde{R}$$

$$\tilde{\varphi}(\tilde{r}) = \frac{-F\frac{k_2}{k_1}(\frac{1}{k_1^2} - \frac{1}{k_2^2})}{\frac{\sinh u}{u} + \frac{k_2}{k_1}\frac{u\cosh u - \sinh u}{v(v+1)}}\frac{u\cosh u - \sinh u}{(v+1)e^{-v}}\frac{e^{-k_2\tilde{r}}}{k_2\tilde{r}} - \frac{F}{k_2^2}\,, \qquad \tilde{r} > \tilde{R}$$

Profile

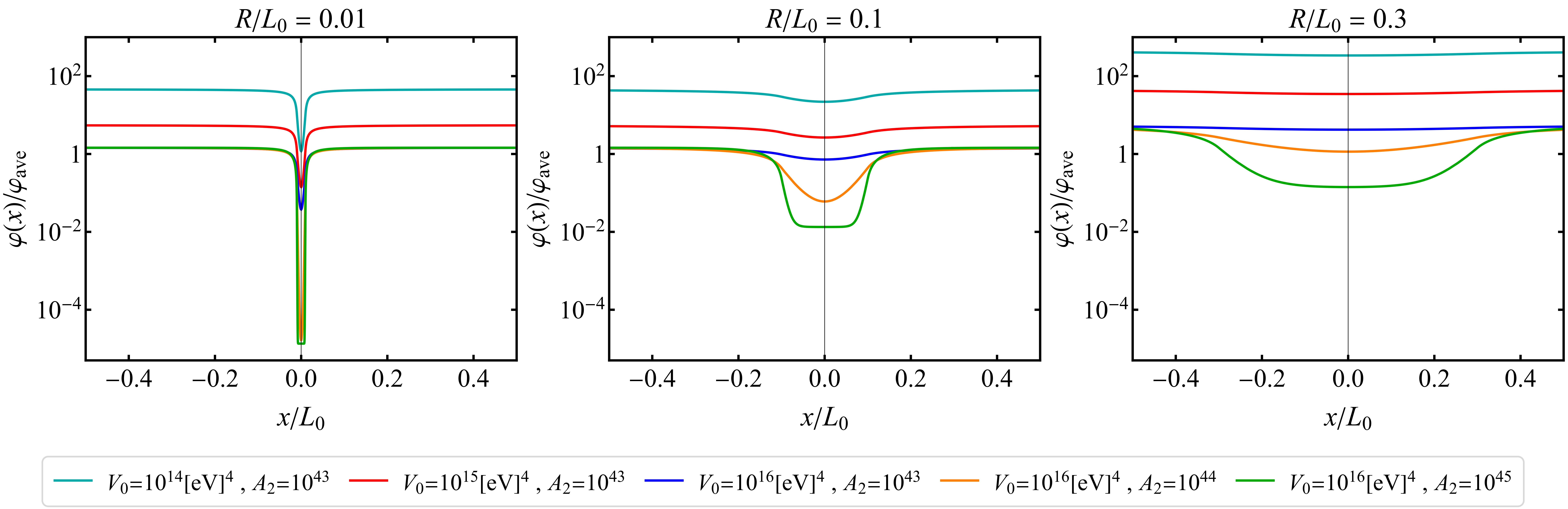

$$\frac{\int_\Omega \varphi(\mathbf{x}) \mathrm{d}^3\mathbf{x}}{\int_\Omega \mathrm{d}^3\mathbf{x}} \equiv \langle \varphi(\mathbf{x}) \rangle_{L_0} = \varphi_0 \langle \tilde{\varphi}(\tilde{\mathbf{x}}) \rangle_1 \,, \qquad z_\phi = \frac{A_2}{2M_{\rm Pl}^2}[\langle \varphi_1(\mathbf{x}) \rangle_{L_0}^2 - \langle \varphi_2(\mathbf{x}) \rangle_{L_0}^2]\,,$$

Material

Material	Osmium	Water	Air	Dilute gas	UHV	XHV	IPM
Mean density $\rho_{\mathrm{ave}}(\mathrm{kg/m^3})$	2.26×10^4	10^3	4.2	4.2×10^{-3}	4.2×10^{-9}	4.2×10^{-15}	4.2×10^{-21}
Particle density $\rho_0(\mathrm{kg/m^3})$	-	-	10^3	10^3	10^3	10^3	10^3
Particle size $R(\mathrm{m})$	-	-	10^{-10}	10^{-10}	10^{-10}	10^{-10}	10^{-10}
Mean distance $L_0(\mathrm{m})$	-	-	10^{-9}	10^{-8}	10^{-6}	10^{-4}	10^{-2}
Reduced size $\tilde{R}$	-	-	10^{-1}	10^{-2}	10^{-4}	10^{-6}	10^{-8}

Two low-density

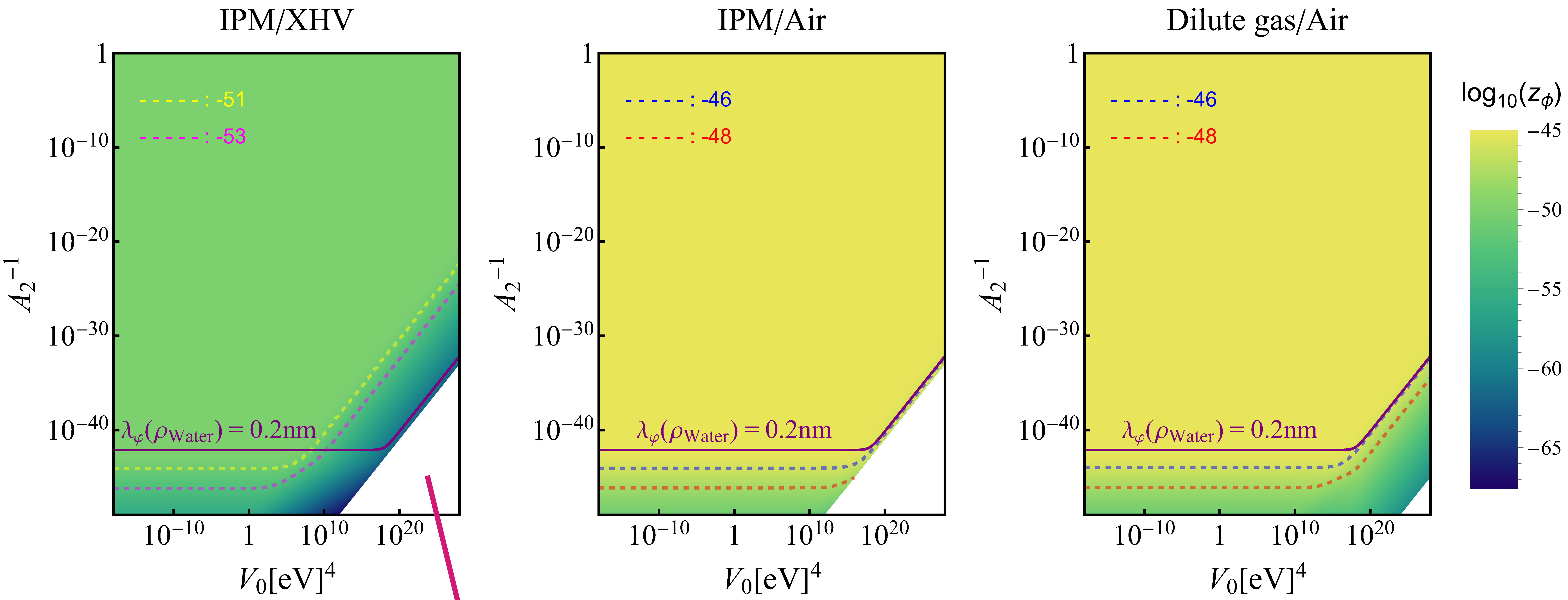

difficulties in numerical integration

[Hu et al., 2509.24622]

Low & high

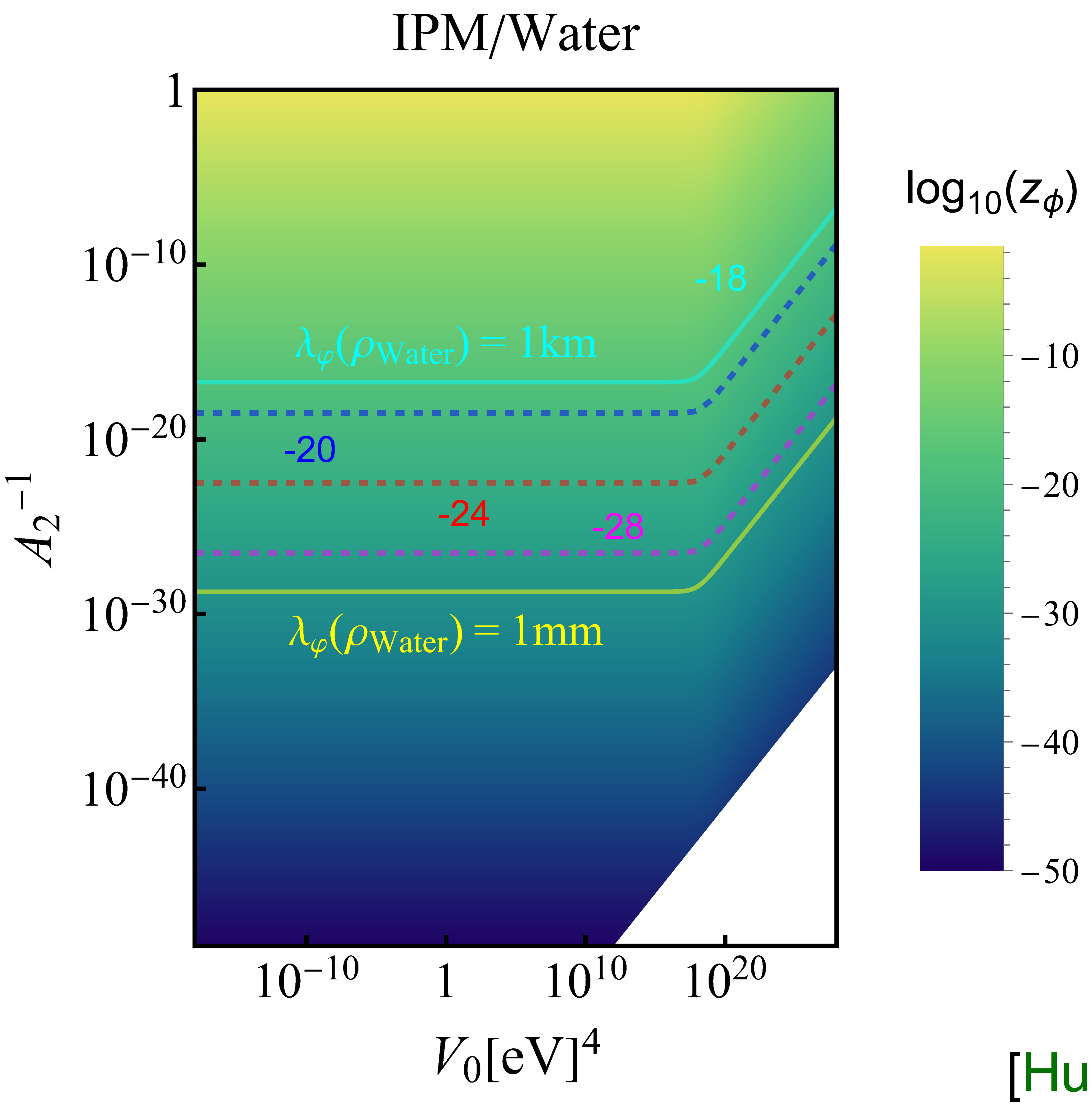

[Hu et al., 2509.24622]

Conclusions & discussions

Continuous model

Increase (decrease) density can detect higher (lower) energy scale

Improving the accuracy of clocks can constrain weaker coupling region

Despite limitations, still quite large regions can rule out in the foreseeable future

Discrete model

One low density (not exceed air), one high density, clocks with accuracy between 10^{-18} and 10^{-30} can constrain the parameter space

Two low density, can not constrain any area with nowadays technology